DE GRUYTER OPEN
Powder Metallurgy Progress, Vol.16 (2016), No.2, p.59-85
http://dx.doi.org/10.1515/pmp-2016-0006

# SINTERED STRUCTURAL STEELS CONTAINING Mn, Cr AND Mo – THE SUMMARY OF THE INVESTIGATIONS

**M. Sulowski**

***Abstract***
*The paper is presented the development and method of production of modern, Ni-free sintered structural steels which contain carbide forming alloying elements (Cr) with high affinity for oxygen (Cr, Mn) and the much smaller additive of an expensive alloying element (Mo), enabling the production of structural sintered steels in commercial belt furnaces, using safe sintering atmospheres. The investigations reported deal with the analysis of microstructure and mechanical properties of these sintered structural steels produced in different processing conditions, especially modification of chemical composition of sintering atmosphere and also the connections between the microstructure of sintered material and its mechanical properties. This analysis was done to propose the appropriate chemical composition of sintered Ni-free steels with properties which are comparable or even better than those of sintered structural steels containing rich and carcinogenic nickel. The investigations of PM Mn-Cr-Mo steels were preceded by those on Mn steels.*
***Keywords: alloying elements, sintering parameters, sintered steels, mechanical properties, microstructure***

## INTRODUCTION

Powder metallurgy (PM) steels are differ significantly from their wrought counterparts. The elements, such as Ni and Cu, and in some cases Mo, are the alloying elements which have traditionally been used in high-strength sintered structural steels. Mn has a significant influence on hardenability but its use is very restricted because of its strong affinity for oxygen. From the Ellingham-Richardson diagram [1] it can assumed that sintering of Mn steels is not practicable in endogas and, even in pure $H_2$, and the dew point requirements for sintering temperatures of 1120°C and 1250°C are –60°C and –50°C, respectively. On the other hand Ni, Cu, and particularly Mo additions are more effective than additions of Mn, because their oxides are reducible during sintering in standard industrial conditions (1120°C, dissociated ammonia atmosphere, –30°C dew point). However, the PM industry follows possibilities of developing Ni-free sintered steels, which render mechanical properties as high as diffusion alloyed Ni-containing sintered steels and further fulfill the requirements of health protection [2].

During last 60 years PM Mn structural steels have been the interests of scientists from all over the world. The main topics of the researches concerned the effect of Mn content and other alloying elements on the mechanical properties of PM structural parts, the effect of alloying elements, allow to create liquid phase during sintering, on the microstructure and mechanical properties of sintered Mn steels and elimination of expensive and carcinogenic Ni and heavy-recycled Cu by introducing in sintered steels Mn and Cr causing to increase the mechanical properties of PM Mn steels [3-10].

Maciej Sulowski, AGH University of Science and Technology, Faculty of Metals Engineering and Industrial Computer Science al. Mickiewicza 30, 30-059 Cracow, Poland

In 1996 Canadian company Stockpole was patented the sintered steel with Mn in excess of 1%. Commercial exploitation of PM Mn ferrous alloys appears restricted to < 1.5% Mn at sintering temperatures < 1300ºC. However, even these Mn contents require special processing procedures to minimise the oxygen level of the starting powders. With a tensile strength of at least 600 MPa, and very good dimensional stability, sintered Mn steels with density about 7 g/cm$^3$ find applications in automotive industry. In Europe in recent years Mn has been very often introduced as an alloying element in Fe-based structural parts [3, 11, 12]. Nowadays, many research centres are dealing with sintered structural Fe-Mn-(Cr)-(Mo)-C steels (i.e. Hoeganeas Corporation, USA [13, 14], Höganäs, AB, Sweden [15], IMR SAS, Kosice, Slovakia [16, 17], Chalmers University of Technology, Department of Materials and Manufacturing Technology, Goteborg, Sweden [18-20], Vienna University of Technology, Institute of Chemical Technologies and Analytics, Vienna, Austria [21]). This work resulted in many publications, presentations and posters presented during PM international conferences and congresses.

## EXPERIMENTAL MATERIALS

During investigations the following powders were used as the starting materials: Höganäs iron powders: grade NC 100.24 and ABC 100.30, Höganäs pre-alloyed iron powders: Astaloy Mo, Astaloy CrL, Astaloy CrM, Ferromanganese powders: Elkem low-carbon ferromanganese (77%Mn, 1.3%C) (Eramet Norway Sauda) and HP III (79% Mn, 6.35% C) delivered by Huta Pokoj, Höganäs graphite powder grade C-UF.

From these powders mixtures with compositions of: Fe-(3-4)%Mn-0.8%C, Fe-(3-4)%Mn-0.5%Mo-(0.6-0.8)%C and Fe-0.5Mo-(0.6-0.8)%C, Fe-3%Mn-(1.5-3)%Cr-(0.2-0.5)%Mo-(0.3-0.8%)C, were double cone and Turbula mixed for 60 and 30 minutes, respectively. Following mixing, green compacts 5x10x55 mm and according to PN-EN ISO 2740 standard were single-action pressed for the same green densities (6.8-6.9 g/cm$^3$) at 660 and 820 MPa, respectively. To minimize friction, zinc stearate was used as a lubricant and was applied on the punches before pressing each sample.

Following pressing, compacts were sintered in a semi-closed container proposed by Cias [22] at: 1120°C, 1150°C, 1180°C, 1200°C with different atmosphere dew point varied from -40°C up to -60°C (Fe-(3-4)%Mn-0.8%C steels), 1220°C (Fe-(3-4)%Mn-0.5%Mo-(0.6-0.8)%C and Fe-0.5Mo-(0.6-0.8)%C steels) – dew point - -60 ºC, 1120°C and 1250ºC (steels based on Astaloy pre-alloyed powders) – dew point - -60ºC, for 60 minutes in pure $N_2$ (quality standard 5.0), pure $H_2$ (quality standard 5.0) and mixtures thereof (from 5%$H_2$ to 75%$H_2$). Heating rate to sintering temperature was 75ºC/min. Three types of heat treatment after sintering were employed: sinterhardening (cooling rate – CR = 66°C/min), sinterhardening (cooling rate CR = 66°C/min) and tempering at TT = 200°C or slow furnace cooling (cooling rate CR = 3.5ºC/min).

## EXPERIMENTAL METHODS

The steels were physically (green and as-sintered densities) and mechanically (tensile, 3-point bend, toughness, apparent hardness and microhardness) tested at room temperature. Green and as-sintered (as-tempered) densities were calculated by the geometric and Archimedes methods. Tensile testing was carried out on a MTS 810 instrument at a cross-head speed of 1 mm/min. Tensile and bend strengths and hardness were calculated according to PN-EN 10002-1 standard. TRS was measured using a ZD10-90 machine, following PN-EN 3325 standard. The load was applied to the surface on which the pressing punch contacted. Hardness was investigated on the macroscale on WPM Vickers / Brinell hardness tester and on the microscale on an Innovatest machine using the

Vickers method. Impact test (KC) was carried out using 55x10x5 mm specimens and a 15 J Charpy bar impact tester according to the PN–EN 10045–1 standard (samples were placed on supports with a distance of 25 mm). The number of tested samples in each batches was 10 (mean value for 10 samples). The standard deviation for each properties was shown in Table 1.

Tab.1. The range of standard deviation for each property of PM Fe-Mn-Cr-Mn-Mo-C steels.

| Sintering temp. °C | UTS MPa | $Rp_{0.2}$ offset, MPa | A % | TRS MPa | KC J/cm$^2$ | Cross and app. HV 10 (HV 30) |
|---|---|---|---|---|---|---|
| 1120 | ±22 ÷ ±70 | ±3 ÷ ±90 | ±0.2 ÷ ±0.4 | ±55 ÷ ±154 | ±0.8 ÷ ±1.5 | ±29 ÷ ±64 |
| 1250 | ±39 ÷ ±79 | ±22 ÷ ±61 | ±0.3 ÷ ±0.7 | ±68 ÷ ±146 | ±1.0 ÷ ±2.1 | ±30 ÷ ±63 |

Following mechanical tests, metallographic (LOM) and fracture investigations (SEM) were carried out using Leica DM 4000M and JEOL JSM 700F instruments, respectively. Samples were prepared according to the procedure described in [23].

## RESULT AND DISCUSSION

### Chemical reaction taking place during sintering of Fe-Mn-C steels

James et al [13] considering Mo steels concluded that the microstructure and properties depend not only on sintering temperature, but also on chemical reactions during heating compacts to the sintering temperature and during isothermal sintering. Because Mn is an alloying element with a high affinity for $O_2$, it is very important to establish the chemical reactions between Mn oxides and the sintering atmosphere. It is important to state at the outset that Mn has a very high vapour pressure, e.g. already $10^{-1}$ mmHg at 1200°C. Investigations [24] show that during sintering Mn steels in $H_2$-containing atmosphere, not only Fe and Mn oxides are reduced, but also decarburization of sintered parts is possible. Responsible for it is the chain of relevant chemical reactions [4, 25-28]:

$Mn[vapour] + H_2O = MnO + H_2$ (1)

$3Fe_2O_3 + H_2 = 2Fe_3O_4 + H_2O$ (2)

$Fe_3O_4 + H_2 = 3FeO + H_2O$ (3)

$FeO + H_2 = Fe + H_2O$ (4)

$C+O_2 = CO_2$ (5)

above 927°C, these chemical reactions are possible:

$C + H_2O = H_2 + CO$ (6)

and accordingly:

$3Fe_2O_3 + CO = 2Fe_3O_4 + CO_2$ (7)

$Fe_3O_4 + CO = 3FeO + CO_2$ (8)

$FeO + CO = Fe + CO_2$ (9)

also the Boudouard reaction:

$C+CO_2 = 2CO$ (10).

Reactions (10) and (6), lead to C loss. The net reaction of (9), (10) and (6) gives:

$FeO + C = Fe + CO$ (11)

to be considered also are these possible reactions:

$3Fe + CO + H_2 = Fe_3C + H_2O$ (12)

$3Fe + 2CO = Fe_3C + CO_2$ (13)

$3Fe + C = Fe_3C$ (14)

$MnO + CO = Mn + CO_2$ (15)
$2C + O_2 = 2CO$ (16)
and the Sabatier reaction:
$CO_2 + 4H_2 = CH_4 + 2H_2O$ (17).
Another reaction leading to C loss is the methane reaction > 1200°C:
$2H_2 + C = CH_4$ (18).
For temperatures above 1200°C, further reactions can take place:
$5MnO + 7C = Mn_5C_2 + 5CO$ (19)
$2MnO + Mn_5C_2 = 7Mn[vapour] + 2CO$ (20).

Accordingly the higher carbon loss after sintering at 1250°C is attributed to the Boudouard reaction, the methane forming and the MnO reduction by carbide reactions (19) and (20). This problem was also raised by Hryha and Nyborg, e. g. in [29].

**The mechanical properties of 3 and 4%Mn PM steels**

The work described in [30] dealt with the establishment of the proper processing parameters for the production of sintered steels containing 3 and 4% of Mn, based on different, commercial iron powders. As the Mn carrier two types of ferromanganese powders: low- and high- carbon ferromanganese were used. The investigations allowed the establishment of the most favourable chemical compositions of the powder mixtures. As a result of further investigations, it was decided to choose the following powders: Höganäs sponge iron powder grade 100.24 and Elkem low-carbon (1.18%C) ferromanganese. The results obtained show the influence of sintering temperature on mechanical properties of the investigated steels (Table 2). During these investigations [30], it was concluded that mechanical properties of PM Mn steels are very close to the properties of Ni PM steels [63], which allows their designation to be high-strength steels. It is worth emphasizing, if cooling rate of these steels from sintering temperature to room temperature produces a bainitic or bainitic-martensitic structure, these steels will be characterized by higher strength. Moreover, less expensive Mn has a stronger effect on the hardenability of steels the than carcinogenic Ni.

Additional work, dealing with the effect of processing parameters on the microstructure and properties of PM Mn steels, was work described in [31]. From [30] it was concluded that increasing the sintering temperature to 1250°C was very important, with the reference temperature 1120°C. The intention was to check if sintered alloyed steels containing alloying elements with a high affinity for oxygen can be produced in a $H_2$-poor atmosphere. Modification of chemical composition of sintering atmosphere was connected with decreasing the amount of $H_2$ in the sintering atmosphere, following this scheme: 100% $H_2$, 75% $H_2$ – 25% $H_2$, 25% $H_2$ – 75% $N_2$, 5% $H_2$ – 95% $N_2$, 100% $N_2$.

Tab.2. Mechanical properties of PM (3-4)%Mn-0.8%C steels sintered in $H_2$ with different dew point [30, 31]

| Sint. temp. °C | Compo-sition | UTS [MPa] | | A [%] | | TRS [MPa] | | KC [J/cm²] | | Apparent cross-sectional hardness HV 10 | |
|---|---|---|---|---|---|---|---|---|---|---|---|
| | | –40°C | –60°C | –40°C | –60°C | –40°C | –60°C | –40°C | –60°C | –40°C | –60°C |
| 1120 | NC 100.24 + Elkem Fe-3Mn-0.8C | 451[a] | 432[a] | 0.68[a] | 0.58[a] | 976[a] | 1242[a] | 8.34[a] | 7.94[a] | 203[a] | 214[a] |
| 1150 | NC 100.24 + Elkem Fe-3Mn-0.8C | 384[a] | 427[a] | 0.29[a] | 0.29[a] | 1236[a] | 1254[a] | 6.09[a] | 7.62[a] | 216[a] | 183[a] |
| 1180 | NC 100.24 + Elkem Fe-3Mn-0.8C | 400[a] | 583[a] | 0.16[a] | 0.72[a] | 832[a] | 1253[a] | 3.72[a] | 7.22[a] | 132[a] | 196[a] |
| 1200 | NC 100.24 + Elkem Fe-3Mn-0.8C | 468[a] | 445[a] | 0.26[a] | 0.31[a] | 1240[a] | 1015[a] | 3.49[a] | 5.45[a] | 351[a] | 266[a] |
| 1120 | NC 100.24+ Elkem Fe-4Mn-0.8C | 340[a] | 368[a] | 0.25[a] | 0.40[a] | 1124[a] | 968[a] | 3.09[a] | 3.63[a] | 284[a] | 222[a] |
| 1150 | NC 100.24+ Elkem Fe-4Mn-0.8C | 328[a] | 345[a] | 0.35[a] | 0.24[a] | 884[a] | 840[a] | 2.31[a] | 3.17[a] | 264[a] | 298[a] |
| 1800 | NC 100.24+ Elkem Fe-4Mn-0.8C | 298[a] | 306[a] | 0.15[a] | 0.09[a] | 811[a] | 771[a] | 2.43[a] | 2.17[a] | 331[a] | 351[a] |
| 1200 | NC 100.24+ Elkem Fe-4Mn-0.8C | 321[a] | 289[a] | 0.08[a] | 0.13[a] | 789[a] | 745[a] | 2.52[a] | 2.21[a] | 288[a] | 372[a] |
| 1200 | NC 100.24 + HP III Fe-3Mn-0.8C | - | 420[a] | – | 0.26[a] | – | 835[a] | – | 4.89[a] | – | 211[a] |
| 1200 | NC 100.24 + HP III Fe-4Mn-0.8C | – | 312[a] | – | 0.27[a] | – | 590[a] | – | 3.93[a] | – | 160[a] |
| 1180 | ABC 100.30 + Elkem Fe-3Mn-0.8C | – | 319[a]<br>467[b] | – | 0.18[a]<br>1.82[b] | – | 719[a]<br>1079[b] | – | 2.85[a]<br>9.25[b] | – | 289[a]<br>134[b] |
| 1180 | ABC 100.30 + Elkem Fe-4Mn-0.8C | – | 256[a]<br>479[b] | – | 0.15[a]<br>1.09[b] | – | 415[a]<br>865[b] | – | 3.06[a]<br>3.06[b] | – | 183[a]<br>147[b] |
| 1180 | ABC 100.30 + HP III Fe-3Mn-0.8C | – | 339[a]<br>455[b] | – | 0.52[a]<br>1.82[b] | – | 741[a]<br>868[b] | – | 4.43[a]<br>6.20[b] | – | 205[a]<br>134[b] |
| 1180 | ABC 100.30 + HP III Fe-4Mn-0.8C | – | 285[a]<br>490[b] | – | 0.12[a]<br>1.05[b] | – | 598[a]<br>1021[b] | – | 2.08[a]<br>6.36[b] | – | 233[a]<br>163[b] |

(a) convective cooling (66°C/min); b) furnace cooling (3.5°C/min)

**The effect of cooling rate and tempering temperature on microstructure and mechanical properties of Mn PM steels**

In [31] were described the effects of cooling rate from the sintering and the tempering temperature on the microstructure and mechanical properties of PM alloyed Mn steels. The results obtained in [31] show that compacts based on low carbon ferromanganese reach higher compressibility. Investigations described in [31] show that mechanical properties of sintered steels, especially UTS and TRS, increase with decreasing dew point of the sintering atmosphere. Decreasing of sintering atmosphere dew point allows an increase of toughness and surface hardness of the investigated steels (Table 2). The changes of the sintering atmosphere dew point was carried out using special furnace for removing $O_2$, silica gel, palladium catalysator, molecular sieves and cirogenic cooler. The results show that mechanical properties of sintered structural steels depend on Mn concentration and on cooling rate from the sintering temperature.

Tab.3. Mechanical properties of Fe-3Mn-0.8C PM steels; sintering atmosphere - 100% $H_2$, dew point -60°C [31]

| Composition | 1120°C | | | | | | |
|---|---|---|---|---|---|---|---|
| | CR [°C/min] | UTS [MPa] | TRS [MPa] | HV30 cross. | KC [J/cm$^2$] | $Rp_{0,2}$ offset [MPa] | A [%] |
| NC 100.24 + Elkem + C-UF Fe-3Mn-0.8C | 5 | 478 | 1272 | 224 | 17.22 | 380 | 3.04 |
| | 9 | 506 | 1230 | 217 | 10.86 | 414 | 3.08 |
| | 16 | 568 | 1195 | 248 | 11.06 | 461 | 3.26 |
| | 30 | 557 | 1124 | 272 | 8.22 | 516 | 2.76 |
| | 47 | 559 | 1100 | 276 | 5.84 | 478 | 2.51 |
| | 55 | 535 | 954 | 292 | 5.24 | 518 | 2.01 |
| | 67 | 475 | 1066 | 301 | 4.68 | 528 | 1.90 |
| | 1250°C | | | | | | |
| | CR [°C/min] | UTS [MPa] | TRS [MPa] | HV30 cross. | KC [J/cm$^2$] | $Rp_{0,2}$ offset [MPa] | A [%] |
| | 5 | 595 | 1327 | 254 | 11.50 | 461 | 3.80 |
| | 9 | 614 | 1311 | 239 | 9.92 | 477 | 2.87 |
| | 20 | 583 | 1210 | 265 | 7.66 | 511 | 2.42 |
| | 32 | 586 | 1193 | 282 | 9.38 | 545 | 2.22 |
| | 41 | 521 | 1080 | 328 | 4.59 | 442 | 1.96 |
| | 57 | 491 | 1087 | 335 | 4.92 | 404 | 1.62 |
| | 64 | 458 | 1060 | 301 | 5.04 | 477 | 1.46 |

CR – cooling rate

Cooling rate had a great influence on UTS, TRS, toughness and surface hardness (Table 2). As data show [31], decreasing of cooling rate from sintering temperature sometimes increases mechanical properties by a factor of up to two. The results show that slow cooling rate favours plasticity of sintered steels; elongation after tensile test was about 3.8%, which in the case of sintered steels is a more than satisfactory value (Table 3). It can be concluded that with increasing the sintering temperature, not only are mechanical properties increased, but also plastic properties. Elongation after tensile test of investigated sintered steels increased with decrease of sintering atmosphere dew point and lowering of the cooling rate from the sintering temperature. The use of different tempering temperatures indicated how to make the best and the cheapest product, as to heat treatment. Mechanical properties of these steels, after tempering at 200 and 400°C, were comparable. It can be assumed that increasing the tempering temperature does not favour increase of mechanical properties. Moreover, after tempering at 300°C, mechanical properties if investigated steels decreased, what is probably connected with 300°C embrittlement.

The aim of work described in [31] was also to show if sintering of structural steels containing element(s) with high affinity for oxygen is possible in an atmosphere with a low amount, or even free, of hydrogen. As the results showed (Table 4), mechanical properties of steels sintered in low- $H_2$ or $H_2$-free atmospheres are high. It can be concluded that the change in the chemical composition of the sintering atmosphere is possible - from pure $H_2$ (which is needed for oxide reduction) with low dew point to cheap and safe $N_2$-rich atmosphere and sintering of the investigated steels in $N_2$-rich atmospheres does not decrease significantly their mechanical properties.

Tab.4. Mechanical properties of Fe-3Mn-0.8C PM steels [31].

| Sintering temperature = 1120°C, dew point -60°C, Tempering temperature = 200°C | | | | | | | | |
|---|---|---|---|---|---|---|---|---|
| Compo-sition | CR [°C/min] | $H_2$ in $N_2$-$H_2$ mixture [%] | UTS [MPa] | TRS [MPa] | HV30 cross. | KC [J/cm$^2$] | $Rp_{0,2}$ offset [MPa] | A [%] |
| NC 100.24 + Elkem + C-UF | 67 | 100 | 642 | 1279 | 236 | 4.68 | 386 | 1.87 |
| | | 75 | 640 | 1291 | 247 | 5.09 | 400 | 1.79 |
| | | 25 | 650 | 1299 | 226 | 7.44 | 420 | 1.78 |
| | | 5 | 657 | 1234 | 186 | 7.27 | 421 | 1.82 |
| | | 0 | 655 | 1259 | 202 | 14.31 | 410 | 1.93 |
| Sintering temperature = 1250°C, dew point -60°C, Tempering temperature = 200°C | | | | | | | | |
| Compo-sition | CR [°C/min] | $H_2$ in $N_2$-$H_2$ mixture [%] | UTS [MPa] | TRS [MPa] | HV30 cross. | KC [J/cm$^2$] | $Rp_{0,2}$ offset [MPa] | A [% ] |
| NC 100.24 + Elkem + C-UF | 64 | 100 | 717 | 1296 | 315 | 5.04 | 426 | 1.60 |
| | | 75 | 749 | 1343 | 295 | 13.30 | 443 | 1.71 |
| | | 25 | 778 | 1411 | 298 | 10.83 | 459 | 1.82 |
| | | 5 | 725 | 1420 | 266 | 12.45 | 451 | 1.67 |
| | | 0 | 776 | 1458 | 260 | 13.23 | 464 | 2.00 |

Microstructure of steels investigated in [31] depended on the sintering temperature. Fine, inhomogeneous microstructure was obtained after sintering at 1120°C. It can be prevented by increasing the sintering temperature. The results obtained present the effect of cooling rate from the sintering temperature on the microstructure of the investigated steels. Slow cooling rate, independently of the sintering temperature, contributed to the formation of pearlitic structure. Increasing the cooling rate resulted in: first fine pearlite, then acicular bainite with martensite, and finally acicular bainite with martensite and retained austenite (Table 5).

Tab.5. Microstructural constituents of Fe-3Mn-0.8C PM steels vs. cooling rate (CR) and sintering temperature (ST) [31].

| CR, [°C/min] | ST = 1120 [°C] | CR, [°C/min] | ST = 1250 [°C] |
|---|---|---|---|
| 5 | Pearlite | 5 | Pearlite + proeutectoid ferrite |
| 9 | | 9 | |
| 16 | Fine pearlite (troostite) | 20 | Fine pearlite + feathery bainite |
| 30 | Feathery bainite + fine pearlite | 32 | Acicular bainite + martensite |
| 47 | Acicular bainite + martensite + Mn-rich austenite | 41 | Acicular bainite + martensite + retained austenite |
| from 55 | Acicular bainite + martensite + retained austenite | from 57 | |

The microstructure of investigated steels depends also on the tempering temperature. Low tempering (200°C) resulted in tempered martensite with retained austenite (and sometimes with bainite) structure. Tempering of steel at 300°C and 400°C caused sorbite formation in the microstructure of steel.

The microstructure of investigated steels, presented in Fig. 1 and 2, depended on the chemical composition of the sintering atmosphere. After sintering in $H_2$, steels were characterised by martensitic structure with retained austenite regions. After sintering in $N_2$, in investigated steels martensitic/bainitic structure (with retained austenite and troostite) or martensite with retained austenite and bainitic regions were observed after sintering at 1120°C and 1250°C, respectively. In investigated steels the presence of 3% Mn caused a slow pearlitic transformation. After cooling with a higher rate (~60°C/min.), microstructure of investigated steels was inhomogeneous, containing martensite, upper or lower bainite, retained austenite and sometimes ferrite. On the other hand, slow cooling rate (3.5°C/min.) favoured plasticity of steels in which pearlitic structure predominated.

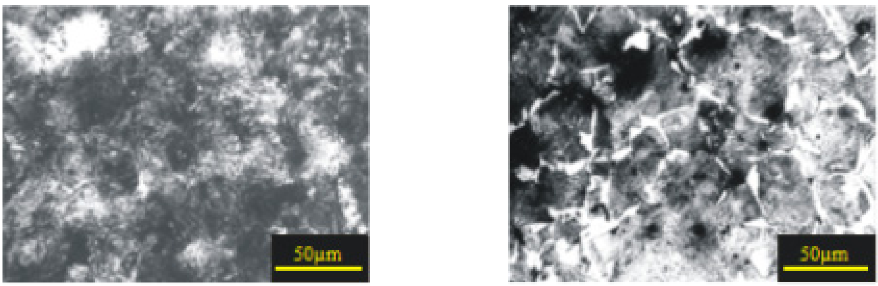


a) b)

Fig.1. Photomicrograph of Fe-3Mn-0.8C PM steels; ATM = 100% $H_2$, DP = - 60°C; CR = 5 and 9°C/min. [31]; a) ST = 1120°C – pearlite, b) ST = 1250°C - pearlite and ferrite.

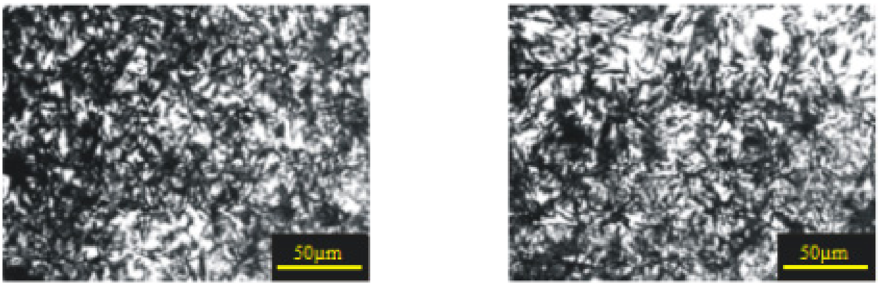


a) b)

Fig.2. Photomicrograph of Fe-3Mn-0.8C PM steels ATM = 100% $H_2$, DP = -60°C [31]; a) ST = 1120°C, CR > 55°C/min – bainite, martensite and retained austenite, b) ST = 1250°C, CR > 57°C/min – bainite, martensite and retained austenite.

PM Mn and Mn-Cr-Mo steels are sinter-hardenable, i.e. can be hardened directly from the sintering temperature with a higher than critical cooling rate. This is possible only for steels containing alloying elements with a high affinity for oxygen. This special composition enables the elimination of additional heat treatment (hardening and tempering), and, as a consequence, the lowering of costs of production of parts made from such steels.

During investigations described in [31] the effect of processing parameters on fracture of Mn PM steels was analysed. From these results obtained it can be concluded that a steel fast cooled from the sintering temperature (60°C/min – sinter-hardened steel) was characterized by transgranular brittle fracture (on tensile curve small, about 0.1% elongation, was observed). Sometimes, because of thin "oxide film", the fracture was intergranular. The use of heat treatment caused changes to fracture of these steels – from brittle to transgranular ductile fracture. In this case (ductile fracture), elongation was up to 4%.

Tab.6. The properties of PM steels - sintering temperature 1220°C [32].

| Chemical composition / sintering atmosphere | UTS, MPa | $Rp_{0,2}$ offset, MPa | A, % | TRS, MPa | HV 30 cross. |
|---|---|---|---|---|---|
| Fe-3Mn-0.6C-0.5Mo-0.03Si / $N_2$ | 639 | 535 | 2.99 | 1253 | 255 |
| Fe-3Mn-0.6C-0.5Mo-0.03Si / $H_2$ | 659 | 453 | 2.70 | 1164 | 250 |
| Fe-3Mn-0.8C-0.5Mo-0.04Si / $N_2$ | 600 | 385 | 2.83 | 1390 | 312 |
| Fe-3Mn-0.8C-0.5Mo-0.04Si / $H_2$ | 635 | 417 | 2.88 | 1205 | 285 |
| Fe-4Mn-0.6C-0.5Mo-0.04Si / $N_2$ | 535 | 385 | 1.60 | 954 | 281 |
| Fe-4Mn-0.6C-0.5Mo-0.04Si / $H_2$ | 564 | 369 | 1.71 | 1092 | 301 |
| Fe-4Mn-0.8C-0.5Mo-0.04Si / $N_2$ | 455 | - | 1.10 | 1032 | 280 |
| Fe-4Mn-0.8C-0.5Mo-0.04Si / $H_2$ | 467 | 384 | 1.23 | 985 | 224 |
| Fe-0.5Mo-0.6C / $N_2$ | 486 | 351 | 2.32 | 982 | 133 |
| Fe-0.5Mo-0.6C / $H_2$ | 466 | 359 | 1.97 | 921 | 165 |
| Fe-0.5Mo-0.8C / $N_2$ | 541 | 383 | 2.34 | 1041 | 151 |
| Fe-0.5Mo-0.8C / $H_2$ | 512 | 350 | 2.14 | 964 | 163 |

Work described in [32] dealt with the possibility of using $N_2$ as an alternative atmosphere for sintering not only Mn steels, but also steels containing Mo [30, 31]. Molybdenum is one of the important alloying elements very commonly used in PM Fe-based materials. The addition of this element to PM steel causes solid solution hardening and increases UTS and hardness without decreasing plastic properties of the steel (Table 6). In this way, Mo, when together with Mn, is a very important factor which decides the hardenability of sintered steels. The synergy effect of Mo and Mn is more pronounced than the individual effects of Mo or Mn.

**PM alloyed steels containing manganese and molybdenum**

Nowadays, sintered steels with the addition of Mn, Mo and Cr are of interest to other researchers. Numerous publications about PM Mn-Cr-Mo steels have been written, for example, by Mitchell, Wronski, Cias [3-4, 7, 9], Keresti [8] Salak [8, 11-12], Hryha [18-20] and Gierl-Mayer [21], The results obtained in [32] enable these materials to be designated as medium-to-high strength steels (UTS = 640 MPa, $Rp_{0.2}$ yield offset = 535 MPa). On the basis of the results obtained in [32], lack of Mn, in the composition of such sintered steels had an unfavourable influence on the properties of the investigated steels. The results show that sintered Mn-Mo steels had a good plasticity, although elongation after tensile test did not exceed 3%. The microstructure of investigated steels was inhomogeneous. The main structural constituents were bainite, martensite and Mo-rich ferrite. The essential observation was that mechanical properties of the investigated steels after sintering in $H_2$ were comparable with those of steels sintered in $N_2$, which confirmed previous investigations [24, 30, 31]. It shows that $N_2$ atmosphere can be a competitive substitution for the expensive and dangerous $H_2$, and it can be used for production of PM steels containing Mn and Mo.

The effect of cooling rate and tin additions on microstructure and mechanical properties of Mn alloyed sintered steels

In [32] the effects of cooling rate from sintering temperature and Sn additions on the microstructure and mechanical properties of PM Mn steels were described. The use of Sn as an alloying element, having favourable influence on the microstructure and properties of Fe-based PM materials, was described in [33-36].

Tab.7. The $Rp_{0.2}$ yield strength and elongation after tensile test, A, of Fe-3Mn-0.8C PM steels sintered in $H_2$ atmosphere with a dew point -60°C [37]

| CR, °C/min | 1120°C | | | 1250°C | | |
|---|---|---|---|---|---|---|
| | UTS, MPa | $Rp_{0,2}$ offset, MPa | A, % | UTS, MPa | $Rp_{0,2}$ offset, MPa | A, % |
| 5 | 478 | 380 | 3.04 | 595 | 461 | 3.80 |
| 9 | 506 | 414 | 3.08 | 614 | 477 | 2.87 |
| 16 | 568 | 461 | 3.26 | 583 | 511 | 2.42 |
| 30 | 557 | 516 | 2.76 | 586 | 545 | 2.22 |
| 47 | 559 | 478 | 2.51 | 521 | 442 | 1.96 |
| 55 | 535 | 518 | 2.01 | 491 | 404 | 1.62 |
| 63 | 498 | 496 | 2.02 | 507 | 560 | 1.82 |
| 64 | 486 | 542 | 2.05 | 500 | ND | 1.75 |
| 67 | 475 | 528 | 1.90 | 458 | 477 | 1.46 |

In [37] the work concentrated on confirming the results described in [33-36] and the possibility of their implementation on an industrial scale. The results show that cooling rate from sintering temperature has a great influence on UTS, TRS, toughness and surface hardness of the investigated steels. Decreasing the cooling rate down to 3.5°C/min sometimes resulted in increases in the mentioned properties by a factor up to two in comparison with properties of steels cooled with higher rates. During the investigations it was found that slow cooling rate favours an increase in plastic properties (Table 7).

Moreover, it was shown that, not only the cooling rate but also the final heat treatment, influence the properties of PM Mn steels. Following the previous work [7, 31], the minimum amount of Mn needed for bainitic/martensitic structure is 3%, whereas carbon concentrations have to be in the range 0.6-0.8%. Following the results presented in [37], during production of high strength sintered steels slow cooling from the sintering temperature is needed. Unfortunately this is possible only on a laboratory scale. When slow cooling rate is employed, it is possible to get in sintered steels pearlitic/lower bainitic structure. These microstructural constituents determine the mechanical properties of steels. On an industrial scale, cooling rate is usually about 10°C/min. Using this rate, bainitic/martensitic or martensitic structure is created in the sintered steel. Steels sintered and cooled with such cooling rate reach high hardness and also high tensile strength (UTS) (see e. g. MPIF Standard 35 – "Materials Standards for PM Structural Parts", published in January 2016). Further increase in mechanical properties can be achieved additionally by heat treatment – tempering at 200°C. Following the data presented in [31], tempering of these steels at 400°C does not increase of mechanical properties. From the data gathered in [37] it can be concluded that to obtain, in PM Mn steels, satisfactory mechanical properties (Tables 2 and 6), which classify them to the group of medium- to-high strength steels, processing variables, especially chemical composition of the powder mixture (controlled Mn content) and cooling rate from the sintering temperature must be keep very tightly.

In [38] the effect of processing variables on the microstructure, porosity and mechanical properties of PM Mn steels was described. The analysis of porosity of investigated materials was carried out on photomicrographs of the microstructure using dedicated software [39]. The values of Equivalent Circular Diameter (ECD) and mean area of pores (Area), calculated for steels sintered at 1250°C were lower than for steels sintered at 1120°C. The results show that there is a difference in total perimeter of pores (Perimeter) after sintering at 1120°C and 1250°C, respectively; these values are very close to each other if slow and rapid cooling was employed (Figs. 3 and 4).

Significantly more internal porosity was observed in samples sintered at 1250°C [38]. As was shown, all measured porosity fraction values for these samples were higher, in the contrast to samples sintered at 1120°C. A reasonable explanation for this could be that Mn is trapped in the closed pores and, after sublimation, the vapours are unable to migrate to the surface due to lack of open pores. These trapped vapours are then preserved as Mn oxides in the compact after cooling. Due to this increase in porosity in samples rapidly cooled after sintering was observed. Efforts were made to mitigate the porosity through a procedural change. The data support the hypothesis that this technique should help to minimise porosity, when Mn is vapourized before pores are closed. Significantly lower porosity was observed in samples made using the furnace-cooling technique.

Sintering at the higher temperature resulted in increasing Shape Factor parameter and mechanical properties of the investigated steels [38]. Low cooling rate favoured porosity. The higher sintering temperature resulted in more rounded porosity and a slight improvement in mechanical properties. Slow cooling rates favoured plasticity. The cooling in the range from 4.5 to 16°C/min produced pearlite with attendant ductility (1.0-1.7%), and strengths up to 595 MPa (tensile) and 1330 MPa (TRS). At higher cooling rates less homogeneous, macroscopically brittle microstructures comprising pearlite, bainite, martensite and retained austenite resulted.

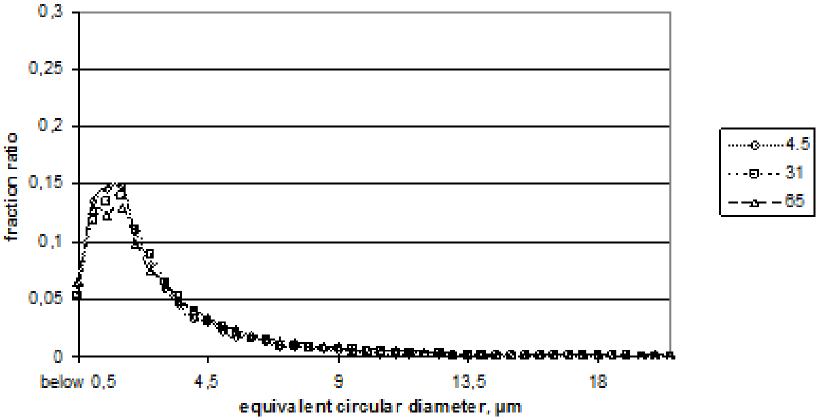


a)

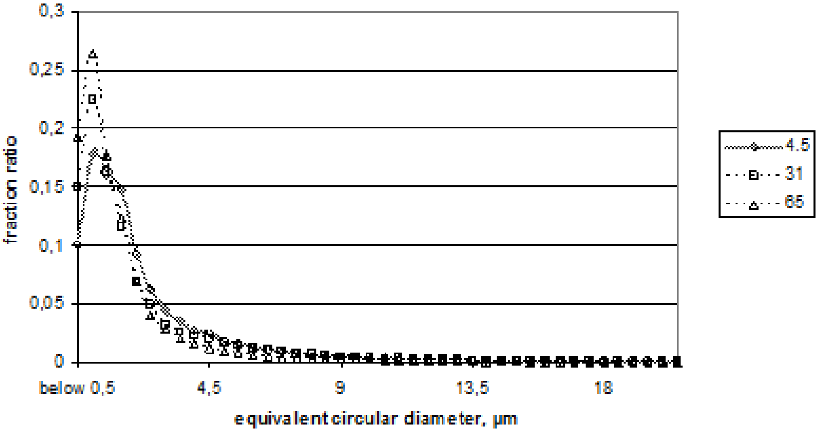


b)

Fig.3. Graphical representation of the equivalent circular diameter distribution for specimens sintered at a) 1120°C and b) 1250°C, cooled with 4.5, 31, and 65°C/min cooling rates [38]

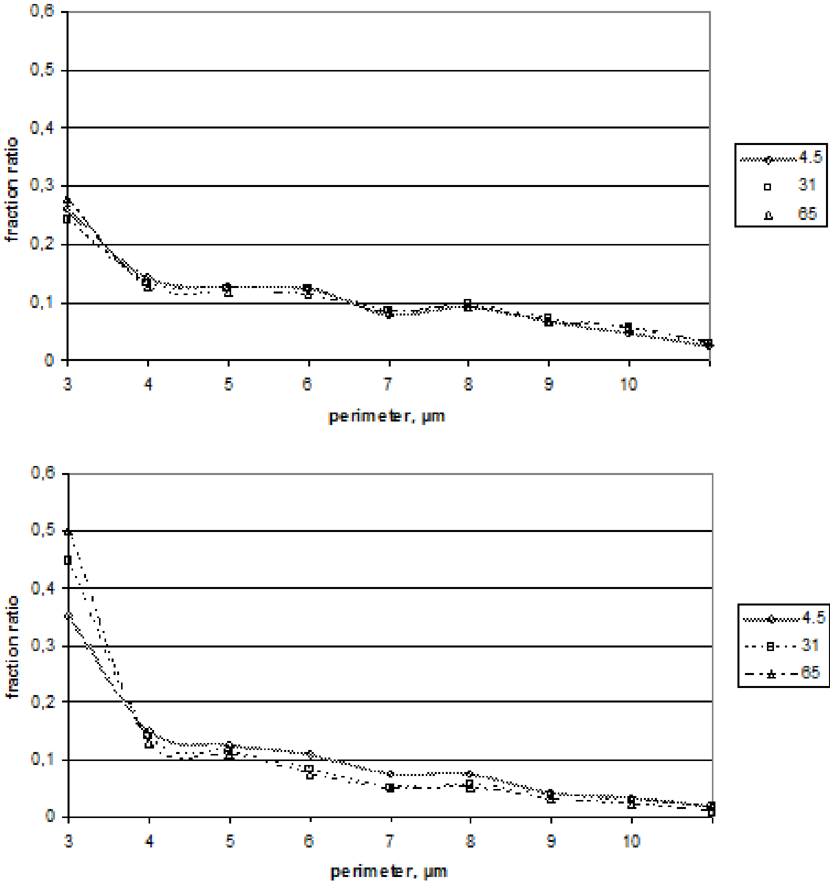


a)

b)

Fig. 4. Graphical representation of the pore perimeter distribution for specimens sintered at a) 1120°C and b) 1250°C, cooled with 4.5, 31, and 65°C/min cooling rates [38].

**Effect of chemical composition of Fe-Cr-Mo-Mn sintered steels**

In [38] chemical composition of PM steels was investigated. As the results show, there is a decarburization effect in the investigated steels (0.2-0.3%). This confirmed the results [40] about the need of addition of extra carbon into the powder mixture to compensate for loosing carbon during the decarburization, which takes place during sintering in an $H_2$-rich atmosphere.

The work described in [41] dealt with non-destructive investigations of sintered structural steels, based on pre-alloyed commercial iron powders alloyed with Cr and Mo. During investigations three methods were employed: High Frequency Ultrasound Echo-Pulse Method, Low Frequency Dynamic Method and Barkhausen Magnetic Noise Method. The results obtained in [41] indicate the heterogeneous nature of investigated materials along the pressing direction. This can affect the toughness of sintered steels. As observed during the investigation, the reduction potential of the sintering atmosphere increased with $H_2$ content in the sintering atmosphere. The strength of investigated steels increased with decreasing concentration of oxides in the steels. The investigations [41] show negligible effect of $N_2$, as a sintering atmosphere, on the strength of investigated steels. The smallest standard deviations – during measurements of the velocity of ultrasonic waves along the pressing direction and Young's modulus – were observed for steels sintered in $H_2$ or $N_2$. Young's modulus of steel based on Astaloy CrL powder, sintered at 1250°C in the mixture of 5%$H_2$ – 95%$N_2$, was characterized by the smallest standard deviation, whereas the biggest was observed for this steel sintered in the mixture of 25%$H_2$ – 75%$N_2$. The smallest Young's modulus was measured in the steel based on Astaloy CrM powder (with higher Cr and Mo contents) after sintering at 1250°C in $N_2$. Young's modulus was in the range 140 to 170 GPa; an insignificant decrease of Young's modulus with increasing sintering temperature was observed. As was confirmed during this work, both the velocity of ultrasound waves and Young's modulus depend on the porosity of sintered material. The results show also a negligible effect of chemical composition of sintering atmosphere on the Barkhausen noise voltage, except for steels based on Astaloy CrM powder, sintered at 1120°C in $H_2$. Investigated steels, both based on Astaloy CrL and Astaloy CrM powders, were characterized by the highest velocity of ultrasonic waves along the pressing direction and the smallest Barkhausen noise voltage. It was also found, in spite of a negligible effect of chemical composition of investigated steels on Young's modulus, that steels with lower Cr and Mo concentrations have a somewhat higher Young's modulus than steels based on Astaloy CrM powder, sintered at the same temperature.

Tab.8. Mechanical properties of Fe-Mn-Cr-Mo-C PM [42].

| Sintering temperature, °C and atmosphere | | UTS, MPa | $Rp_{0.2}$ offset, MPa | A, % | TRS, MPa | KC, J/cm$^2$ | HV 30 surf. |
|---|---|---|---|---|---|---|---|
| Fe-3Mn-1.5Cr-0.2Mo-0.3C | | | | | | | |
| 1120 | 75%$H_2$-25%$N_2$ | 512 | 428 | 1.3 | 907 | 3.2 | 190 |
| | 25%$H_2$-75%$N_2$ | 438 | 361 | 0.9 | 1042 | 2.1 | 207 |
| | 5%$H_2$-95%$N_2$ | 400 | 429 | 0.8 | 691 | 2.2 | 247 |
| | 100 % $N_2$ | 374 | 285 | 0.7 | 922 | 2.0 | 229 |
| Fe-3Mn-3Cr-0.5Mo-0.3C | | | | | | | |
| 1120 | 75%$H_2$-25%$N_2$ | 584 | 498 | 1.1 | 987 | 3.1 | 255 |
| | 25%$H_2$-75%$N_2$ | 532 | 451 | 1.1 | 1036 | 3.0 | 302 |
| | 5%$H_2$-95%$N_2$ | 515 | 386 | 1.0 | 915 | 2.7 | 341 |
| | 100 % $N_2$ | 495 | 479 | 1.0 | 96 | 3.0 | 353 |
| Fe-3Mn-1.5Cr-0.2Mo-0.3C | | | | | | | |
| 1250 | 75%$H_2$-25%$N_2$ | 602 | 398 | 1.6 | 1027 | 4.4 | 260 |
| | 25%$H_2$-75%$N_2$ | 510 | 466 | 1.1 | 1214 | 4.5 | 249 |
| | 5%$H_2$-95%$N_2$ | 456 | 484 | 0.8 | 1148 | 3.0 | 235 |
| | 100 % $N_2$ | 466 | 429 | 1.2 | 970 | 3.0± | 225 |
| Fe-3Mn-3Cr-0.5Mo-0.3C | | | | | | | |
| 1250 | 75%$H_2$-25%$N_2$ | 816 | 587 | 2.5 | 1454 | 5.5 | 326 |
| | 25%$H_2$-75%$N_2$ | 672 | 569 | 1.5 | 1153 | 3.6 | 345 |
| | 5%$H_2$-95%$N_2$ | 572 | 526 | 1.1 | 1041 | 3.7 | 351 |
| | 100 % $N_2$ | 670 | - | 2.0 | 1061 | 2.9 | 362 |

The work reported in [42] was the continuation of [41] and dealt with the effect of processing parameters, especially chemical composition of the sintering atmosphere and the sintering temperature, on the microstructure and mechanical properties of PM Fe-3%Mn-(1.5-3)%Cr-(0.2-0.5)%Mo-0.3%C structural steels. The results of work [42] (Table 8) show both the influence of chemical composition of the sintering atmosphere and sintering temperature on the mechanical properties of PM Mn-Cr-Mo steels.

The metallographic investigations of these steels show mainly bainitic/martensitic structure with austenite regions. From this work [42] the conclusion can be drawn that mechanical properties of investigated steels are rather high. The highest properties were achieved for steels sintered both in $H_2$-rich atmosphere and in $H_2/N_2$ mixtures. The microstructure of PM Mn-Cr-Mo steels consists mainly of martensite, bainite and austenite. The percentage of microstructural constituents depends on the chemical composition of steel, type of sintering atmosphere and sintering temperature. The high frequency ultrasound echo-pulse method can be used to determine the homogeneity of PM samples that are to be subjected to mechanical tests. A pronounced, slight, anisotropy (up to 1-2%), typical for PM parts, was observed. The type of protective atmosphere did not significantly influence Young's modulus, whose value increased with the increase of the sintering temperature from 1120°C to 1250ºC.

Tab.9. Mechanical properties of Fe-Mn-Cr-Mo-C PM steels [43]

| Fe-3%Mn-1.5%Cr-0.25%Mo-0.8%C | | | | | | | | |
|---|---|---|---|---|---|---|---|---|
| Sintering temperature, °C and atmosphere | | UTS, [MPa] | $Rp_{0,2}$ offset, [MPa] | A, [%] | TRS, [MPa] | KC, [J/cm$^2$] | Hardness HV30 measured on: | |
| | | | | | | | Surface | Cross-section |
| 1120 | 100%$N_2$ | 582 | 275 | 4.4 | 1138 | 12.0 | 186 | 213 |
| | 100% $H_2$ | 612 | 292 | 4.2 | 1282 | 11.6 | 195 | 227 |
| 1200 | 100 %$N_2$ | 723 | 267 | 4.2 | 1470 | 8.7 | 257 | 239 |
| | 100 %$H_2$ | 766 | 260 | 4.3 | 1554 | 14.5 | 229 | 265 |
| Fe-3%Mn-3%Cr-0.5%Mo-0.8%C | | | | | | | | |
| Sintering temperature, °C and atmosphere | | UTS, MPa | $Rp_{0,2}$ offset, MPa | A, % | TRS, MPa | KC, J/cm$^2$ | Hardness HV30 measured on: | |
| | | | | | | | Surface | Cross-section |
| 1120 | 100%$N_2$ | 613 | 273 | 4.2 | 1184 | 8.7 | 213 | 232 |
| | 100% $H_2$ | 671 | 284 | 4.2 | 1356 | 10.8 | 214 | 255 |
| 1200 | 100 %$N_2$ | 761 | 281 | 3.6 | 1529 | 12.0 | 248 | 250 |
| | 100 %$H_2$ | 720 | 280 | 3.4 | 1470 | 18.0 | 249 | 241 |

Additions of alloying elements such as Cu and Ni have traditionally been used in sintered steels for many years. Because of expensive and carcinogenic Ni and difficult-to-recycle Cu, it has been decided to replace these elements with Mo, Mn and Cr, in order to increase the mechanical properties of PM Mn steels. As was shown in [43], for higher concentrations of Cr and Mo, sintering at 1200°C in $N_2$ atmosphere had to be employed to improve strength properties. The UTS, TRS, and A values evaluated on specimens sintered at 1200°C were, by 6%, 4% and 6%, higher than the values obtained for specimens sintered at 1120°C. For lower Cr and Mo concentrations, better properties were achieved after sintering in $H_2$ than in $N_2$, irrespective of the sintering temperature (Table 9).

For higher Cr and Mo concentrations there is a negligible influence of sintering atmosphere on oxygen and carbon contents in the sintered steels. There is a slightly stronger effect of the $H_2$ atmosphere on decarburization of the steel, as compared to $N_2$. As was shown in [43], higher sintering temperature promotes oxide reduction in the Fe-3%Mn-

3%Cr-0.5%Mo-0.8%C steel. The microstructure analysis of Fe-Mn-Cr-Mo-C PM steels was carried out on nital etched metallographic specimens in bright field (BF) and differential interference contrast (DIC) conditions. The light microscopy images show evidence of decarburization and higher porosity in the subsurface layer of specimens, irrespective of the sintering conditions (Fig. 5).

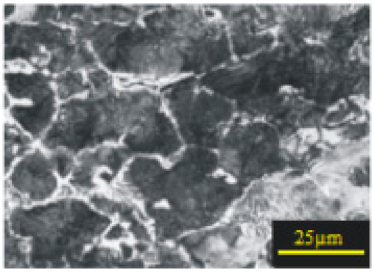


Fig.5. Microstructure of subsurface layer of Fe-3%Mn-3%Cr-0.5%Mo-0.8%C steel, sintered at 1120°C in $N_2$, BF [43].

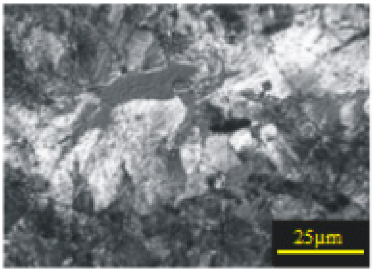


Fig.6. Microstructure of Fe-3%Mn-3%Cr-0.5%Mo-0.8%C steel, sintered at 1120°C in $N_2$, DIC [43].

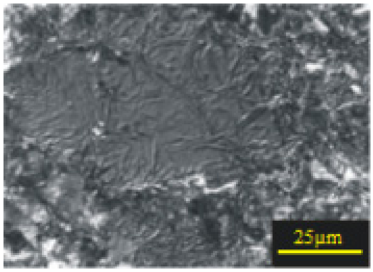


Fig. 7. Microstructure of Fe-3%Mn-3%Cr-0.5%Mo-0.8%C steel, sintered at 1120°C in $N_2$, DIC [43].

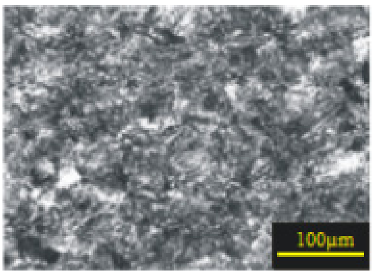


Fig. 8. Microstructure of Fe-3%Mn-3%Cr-0.5%Mo-0.8%C steel, sintered at 1120°C in $N_2$, DIC [43].

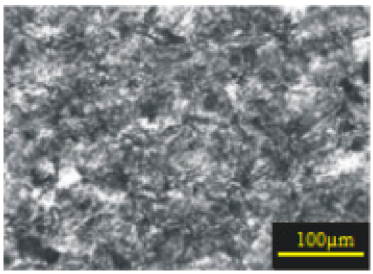


Fig. 9. Microstructure of subsurface layer of Fe-3%Mn-1.5%Cr-0.25%Mo-0.8%C steel, sintered at 1120°C in $N_2$, BF [43].

The steel containing 3% Cr and 0.5% Mo, sintered at 1120°C in $N_2$, has a microstructure consisting of pearlite and bainite (Figs. 6-7). There are few big clusters of tempered martensite and retained austenite, and undissolved particles of ferromanganese and slag inclusions dispersed in a fine-grained microstructure (Figs. 8-9).

The steels sintered at 1200°C contained mainly acicular bainite, tempered martensite and retained austenite, although pearlitic/bainitic regions and undissolved particles of ferromanganese were also observed.

The steels containing 1.5% Cr and 0.25% Mo, based on Astaloy CrL powder, have a more homogeneous microstructure. After sintering at 1120°C in $N_2$, ferritic/pearlitic regions in the subsurface were localised (Fig. 9), whereas the core of the specimens consisted of fine pearlite and bainite (Figs. 10-11). Increasing the sintering temperature did not influence the structure of the investigated steels.

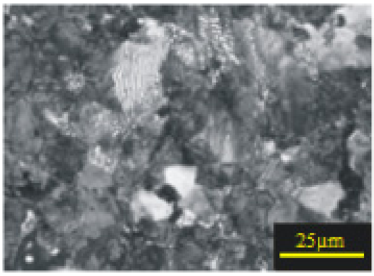


Fig. 10. Microstructure of Fe-3%Mn-1.5%Cr-0.25%Mo-0.8%C steel, sintered at 1120°C in $N_2$, BF [43].

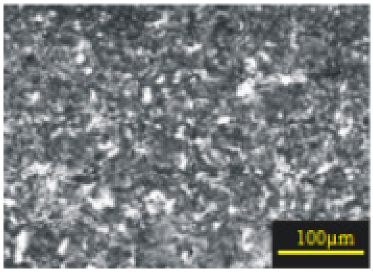


Fig. 11. Microstructure of Fe-3%Mn-1.5%Cr-0.25%Mo-0.8%C steel, sintered at 1200°C in $N_2$, BF [43].

Steels sintered at 1120°C in $H_2$ show coarser microstructures containing pearlite, bainite and troostite (Fig. 12), as well as - after sintering at 1200°C - tempered martensite and retained austenite (Fig. 13). The qualitative metallography confirmed that Mn has been dissolved in the Cr-Mo alloy during sintering and has affected the microstructure formation on cooling.

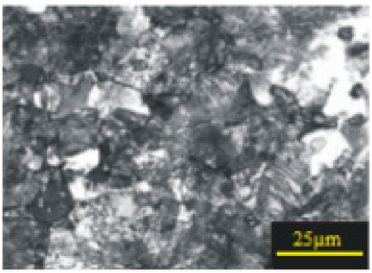


Fig. 12. Microstructure of Fe-3%Mn-3%Cr-0.5%Mo-0.8%C steel, sintered at 1120°C in $H_2$, BF [43].

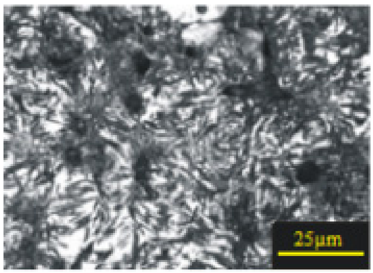


Fig. 13. Microstructure of Fe-3%Mn-3%Cr-0.5%Mo-0.8%C steel, sintered at 1120°C in $H_2$, BF [43].

The mechanical strength results showed a negligible effect of sintering atmosphere on mechanical properties of the investigated steels. It means that Mn-Cr-Mo steels can be successfully processed in a $N_2$-rich atmosphere without decreasing their mechanical properties, as compared to steels sintered in hydrogen. Results obtained from both tensile and bend tests showed a measurable effect of sintering temperature on strength and ductility of the sintered steel, irrespective of the alloy composition and sintering atmosphere.

The work described in [44] concentrated on comparison of mechanical properties of 3%Mn-(1.5-3)%Cr-(0.2-0.5)%Mo-(0.3-0.8)%C PM steels. Additionally reported in this paper are dilatometric investigations. During these tests specimens were observed to expand below $B_s$ and $M_s$ as a result of transformation during cooling at 20 $Kmin^{-1}$. Uninterrupted cooling produced a mixture of bainite and martensite areas. Bainite transformation began at about 450 - 500°C and continued during cooling (Table 10). Martensitic transformation was not always complete before interruption of the dilatometric test. If specimens were sintered in the dilatometer and cooled at 20 $Kmin^{-1}$, bainitic/martensitic transformation occurred during this cooling, to result in mainly martensite, bainite and austenite (also retained austenite) microstructures.

Tab.10. Continuous cooling transformation temperatures established by dilatometric analysis [44].

| Sintering temperature [°C] | Carbon content [%] | 3%Mn + CrL | 3%Mn + CrM |
|---|---|---|---|
| | $F_s$ ; $P_s$ ; $B_s$ transformation temperature [°C] | | |
| 1120 | 0.3 | $F_s$ ; $P_s$ = 850; 650 | $B_s$ ~500 |
| | 0.6 | $B_s$ ~500 | $M_s$ <200 |
| | 0.8 | $B_s$ ~450 | $M_s$ <200 |
| 1250 | 0.3 | $F_s$ ; $P_s$ = 800;700 | $B_s$ ~500 |
| | 0.6 | $B_s$ ~500 | $B_s$ ~500 |
| | 0.8 | $B_s$ ~450 | $B_s$~450 |

Tab.11. Mechanical properties of CrL- and CrM based sintered steels [44].

| Sintering °C | Atm. | min. | UTS, MPa | A, % | $Rp_{0,2}$ offset, MPa | TRS, MPa | KC, $J/cm^2$ | UTS, MPa | A, % | $Rp_{0,2}$ offset, MPa | TRS, MPa | KC, $J/cm^2$ |
|---|---|---|---|---|---|---|---|---|---|---|---|---|
| | | | 3%Mn+CrL+0.3%C | | | | | 3%Mn+CrM+0.3%C | | | | |
| 1120 | $H_2$ | 60 | 566 | 0.80 | 481 | 966 | 3.37 | 462 | 0.58 | 357 | 797 | 5.82 |
| | $N_2$ | | 556 | 0.82 | 481 | 995 | 3.40 | 716 | 2.53 | 535 | 1335 | 4.05 |
| 1250 | $H_2$ | 60 | 608 | 1.16 | 474 | 1279 | 15.18 | 818 | 1.80 | 594 | 1492 | 6.55 |
| | $N_2$ | | 832 | 1.98 | 554 | 1325 | 15.25 | 957 | 2.75 | 562 | 1932 | 10.71 |
| | | | 3%Mn+CrL+0.6%C | | | | | 3%Mn+CrM+0.6%C | | | | |
| 1120 | $H_2$ | 60 | 514 | 1.51 | 473 | 738 | 3.49 | 580 | 1.83 | 435 | 886 | 4.94 |
| | $N_2$ | | 544 | 1.50 | 539 | 1270 | 2.64 | 481 | 1.37 | 412 | 855 | 5.12 |
| 1250 | $H_2$ | 60 | 729 | 2.68 | 547 | 1516 | 7.26 | 968 | 4.37 | 603 | 1734 | 11.22 |
| | $N_2$ | | 728 | 2.31 | 481 | 1503 | 4.27 | 925 | 4.00 | 548 | 2034 | 5.13 |
| | | | 3%Mn+CrL+0.8%C | | | | | 3%Mn+CrM+0.8%C | | | | |
| 1120 | $H_2$ | 60 | 474 | 1.53 | 440 | 989 | 3.79 | 431 | 1.36 | 405 | 956 | 3.50 |
| | $N_2$ | | 431 | 1.18 | 474 | 950 | 3.34 | 389 | 1.31 | 360 | 929 | 4.51 |
| 1250 | $H_2$ | 60 | 704 | 3.29 | 583 | 1435 | 8.25 | 887 | 4.56 | 536 | 1644 | 7.71 |
| | $N_2$ | | 684 | 2.58 | 432 | 1335 | 5.24 | 671 | 2.58 | 517 | 1303 | 8.63 |

In [44] TRS shoved higher values than UTS. It is well-recognised that the value of TRS can exceed that of UTS of the same PM material, identically processed, by a factor up to ~2, although both these parameters relate to the tensile stress causing fracture (Table 11). The analysis of this phenomenon takes account of the pre-failure plastic strain, and enables conversion of the nominal strengths, UTS and TRS, to true fracture stresses [45].

Tensile and three point bend testing was used to determine alloy strength and ductility properties of the steels, but there is concern that testing of standard ISO 2740 specimens may not provide an accurate indication of actual sintered part performance. Part of the basis for this concern is that the thermal processing conditions experienced during laboratory experiments may not be accurately reproduced in industrially produced parts. This means that the mass transport conditions that occur in the laboratory specimens and influence their properties are unlikely to be reflected in industrial furnace processing. Impact strengths in the as-sintered and tempered condition were more dependent upon the sintering temperature than the tensile properties [44].

Compared with the data recorded for the 3%Mn+CrL specimens, the 3%Mn+CrM data showed slightly higher tensile and bend strengths. Also, the yield strength, determined for the 3%Mn+CrM steels, was higher than that of the 3%Mn+CrL alloys, reflecting higher Cr content values.

Generally speaking, the various types of microstructure have been observed in various proportions in all the steels examined [44]. The as-sintered structures consisted of bainite and austenitic/martensitic particles. Optical microscopy investigations show also complex microstructures composed of bainite surrounding a large number of small, substantially unaligned, austenitic/martensitic areas, which are partially decomposed to carbide and ferrite. Austenite grain boundaries are visible. The microstructure is coarser after sintering at 1250°C. In both cases, the austenite regions are typical when they are observed at very high magnifications; the grains are relatively small.

The difference between microstructures obtained by cooling at the same rates after sintering at 1120°C and 1250°C could account for the observed differences in mechanical properties. Alloying elements play an appreciable role in determining the morphology of these microstructures. Thus, the high-Mn and the high-Cr regions in 3%Mn+CrM steel usually exhibit microstructures comprising long coarse plates with these transformed regions extending across prior austenite grains. On the other hand, the microstructure is less acicular in the 3%Mn+CrL steel and grows along the grain boundaries.

As was shown during investigations [45], for higher Cr and Mo concentrations, high temperature sintering in $N_2$ has to be employed to improve strength properties. Recorded values for UTS, elongation and TRS after sintering at 1250°C were higher than those after low temperature processing. These values correspond well to the bainitic/martensitic structure of PM steels. What is more, there is no evident percentage differences between sintering in $H_2$-rich and pure $N_2$ atmosphere. For lower Cr and Mo concentrations, slightly better properties were recorded after sintering in $H_2$-rich than in $N_2$ atmosphere, irrespective of the sintering temperature. Young's modulus evaluated by the supersonic method along the sample was in the range of 144-151 GPa. When we look at plasticity and hardness of Mn-Cr-Mo PM steels, the same tendency as in strength properties can be observed. It can be also pointed out the relatively high elongation – up to 2.5%, which corresponds well with the impact toughness.

It was found in [46] that the steel microstructure strongly depends on the cooling rate after sintering. Bainitic or bainitic/martensitic structure was formed during cooling at 30°C/min and 20°C/min after sintering at 1120°C and 1250°C, respectively. In general, the bainitic structure is relatively acicular and much finer than the pearlitic. This accounts for the improved bend and tensile properties. In investigated steels bainite consists of an aggregate of acicular ferrite and carbides. Its morphology changes progressively with the transformation temperature, i.e. the grain size and acicularity of the microstructure increases as the temperature decreases. The upper bainite comprises larger ferrite plates bounded by $Fe_3C$ precipitates that form directly from the austenite. These microstructures consisted of fine bainite and Mn-rich retained austenite zones, partly transformed into martensite, that do not necessarily contain carbides. When long austenitic-martensitic plates extend across the grains, the impact strength sharply decreases. Finally, a spectacular strength increase along with a marked decrease in impact strength is observed in most specimens when a certain amount of acicular martensite is formed inside the acicular-bainitic regions at the end of the bainitic transformation. Continuous cooling results in a mixture of upper and lower bainitic structures unless the transformation is substantially suppressed by the prior occurrence of the equilibrium, pearlitic transformation.

Chemical analysis using Leco instruments was employed to check the carbon and oxygen contents of the investigated steels. The results obtained confirm decarburisation on the surfaces of the investigated steels. The higher carbon loss, of 0.11%, was recorded for CrM samples sintered at 1250°C in an atmosphere with $H_2/N_2$ ratio 3:1.

Metallographic examinations showed that specimens with lower Cr and Mo contents, sintered at 1120°C, show a bainitic/martensitic structure, whereas in those containing more Cr and Mo, martensitic/austenitic structures are mainly observed. After sintering at 1250°C, the microstructure consists mainly of martensite and bainite regions with small amount of austenite.

## SUMMARY OF THE RESULTS

Till now the majority of sintered structural alloy steels contained nickel, a strongly carcinogenic element (category 3). European Council Directives, strongly advise against using this metal, especially in a strongly dispersed form. In the investigated steels, Cr, Mo and Mn were used as a substitution for Ni. During the whole research, the route of sintering PM steels in semi-closed container, the microatmosphere effect, was employed. This technique, developed and theoretically described – mainly in case of simple Mn steels - by Cias and Mitchell [47] makes possible use of non-explosive and not toxic inert atmospheres in the furnace chamber.

During carrying out the work, the following sintering atmospheres were used: $H_2$, mixture of $H_2$ and $N_2$ with different $N_2/H_2$ ratios and pure $N_2$ (described in [24, 31-32, 37-38, 41-44, 46-51]). To decrease the cost production, an attempt was made to sinter Mn-Cr-Mo steels in air [52], what was novum. (To compare the results, argon as sintering atmosphere was also employed [48]). The analysis of Ellingham-Richardson diagram [45] shows that an atmosphere with extremely low dew point does not ensure, during sintering at 1150°C, protection of Cr and Mn from oxidation. It means that thin film oxides are created in the microstructure, rapidly decreasing the strength of sintered part. Metal oxide will thermally dissociate during sintering in an atmosphere with a given partial oxygen pressure at a given temperature.

The aim of this cycle of investigations was to demonstrate that sintering of Mn-Cr-Mo steels can be carried out in old furnaces using the effect of local microatmosphere, obtained when the compacts are in a semi-closed container [5], because of the gettering effect of Mn vapours and reduction of oxides by carbon monoxide, $H_2$ and active carbon. The microatmosphere which exists in this volume/space during sintering of Mn-containing steels is characterized by a high vapour pressure of this element and the presence of products of carbothermic reactions. This allows a decrease in the $pCO_2/pCO$ and $pH_2O/pH_2$

partial pressure ratios (dew point). It is very important to get locally high carbon potential in the sintering microatmosphere. It can be done by carbothermic reactions with graphite, contained in the green compacts. Carbon, which reacts with metal oxides, carbon dioxide and water vapour, creates in sintering temperature a protective microatmosphere, rich in carbon monoxide and $H_2$. For temperatures above 900°C, carbon monoxide is, relative to Fe, Cr and Mn oxides, a better reducing agent than $H_2$, which is more effective at lower temperatures. Manganese vapours protect the sintered material from oxidation even during heating, in the critical temperature range lying below the sintering temperature. This is a very important observation because at these temperatures the redox reaction is moved towards metal oxidation [24]. This is concluded both from thermodynamic calculations and from the analysis of Ellingham-Richardson diagram [53]. The beneficial result is due to the effect of Dalton's partial pressure law, and also the behaviour of Mn vapour as a getter, which collects the oxygen present in the sintering atmosphere (following A. Salak [54]). Finally, Mn, Mn-Cr and Mn-Cr-Mo steels can be successfully sintered in the technical $N_2$ atmosphere [46, 48, 55, 56] only if semi-closed containers can be used. The positive results with ferromanganese and carbon, added in the form of graphite [57] and the results of investigations of the effect organic substances [10, 58-61] on the microstructure and mechanical properties show the need of such investigations.

Mn-Cr-Mo steels can be processed in low-$H_2$ atmospheres or even in a $N_2$ atmosphere. The mechanical properties of these steels obtained after sintering in such conditions are comparable with, or even better than, mechanical properties of steels sintered in an $H_2$-rich atmosphere. This can be related to the evaporation of Mn and creation of "microclimate" in the boat in which the samples are sintered. The evaporated Mn creates a "cloud" which protects the sintered samples from oxidation and simultaneously is a reducing agent for oxides present in the sintered compacts [62]. To adapt this phenomenon into mass production scale, sintering of Mn-Cr-Mo steels should be carried out in semi-hermetic container and/or with a getter. Following the results obtained [5], sintering of these steels is also possible in a container with a labyrinth seal in the presence of $Al_2O_3$ + Mn + C getter.

In mass production, sintering process is carried out for 30 or 60 minutes [1, 63-64]. Following sintering, sintered compacts are cooled to room temperature. Because the investigated Mn-Cr-Mo steels contained alloying elements strongly influencing hardenability, during processing an additional heat treatment – tempering at 200°C for 60 min. - was employed. This treatment increased their mechanical properties by up to 30% [44, 65].

According to the results of mechanical properties of investigated Mn-Cr-Mo steels, it can be assumed that increasing sintering time increases strength properties of steels based on Astaloy CrL (Fe-1,5%Cr-0.2Mo) and Astaloy CrM (Fe-3%Cr-0.5%Mo). Astaloy CrM-based steels, especially after sintering at the higher temperature, were characterized by better properties compared to Astaloy CrL-based steels (e.g. TRS after sintering for 15 min. – 976 MPa and 1359 MPa, TRS after sintering for 60 min. - 1065 MPa and 1211 MPa for Astaloy CrL and Astaloy CrM-based steels, respectively). Higher mechanical properties of sintered steels based on Astaloy CrM pre-alloyed iron powder were connected with higher Cr and Mo concentrations in the steels [66].

Sintered Mn-Cr-Mo steels are intended for structural parts (e.g. gears in electromachines). They are characterized by high mechanical properties and low friction coefficients. During wear test investigations [67], different friction coefficients have been obtained. The reason was probably structural inhomogeneity of investigated sintered materials. After sintering at 1120°C and 1250°C for 60 min., investigated steels reached friction coefficient of $\mu$ = 0.28-0.38, except for compacts based on Astaloy CrM powder sintered at 1120°C ($\mu$ = 0.54). The increase of friction coefficient could be connected with "sticking on" old layers on the surface of samples during the test. Increasing sintering time up to 180 minutes caused a decrease in structural inhomogeneity of sintered materials and, as a consequence, friction coefficient at the level 0.48.

The obtained results allowed statistical analysis of mechanical properties of sintered steels relating dependence on carbon concentration and tempering time [68]. This analysis shows that fitting curves are 3rd degree polynomials with $R^2$ equal to 1. It is connected probably with small amounts of counting points. Statistical analysis of dependence of properties of sintered materials on the chemical composition of the sintering atmosphere show that fitting curves are 4th degree polynomials or higher with determination coefficient $R^2$ close to 1. The properties depend logarithmically on sintering time. The slopes of the test curves are all equal [68]. The comparison of mechanical properties of PM Mn-Cr-Mo steels produced in different conditions shows that parameters responsible for reproducibility of steel properties are small inhomogeneity of microstructure and structural constituents present in the steels [69].

During metallographic investigation of sintered steels an attempt was made to discover the relationship between processing variables and the microstructure of PM Mn-Cr-Mo steels. The investigations showed that these sintered steels were characterized by high structural inhomogeneity. The microstructural constituents were ferrite, pearlite, upper and acicular bainite, austenite and martensite, and the influence of the structural microconstituents depended on the chemical composition of sintered steels and their processing parameters [31, 37, 70].

The structural inhomogeneity of the investigated steels was confirmed also by examination of elemental distribution [67, 71]. Manganese is an element which closes the ferritic region and creates solid solution with $Fe_g$ in a wide concentration range. On the other hand, Cr and Mo close the austenitic region and create solid solutions with $Fe_a$. Because of relatively low Mo concentration in the investigated steels, sometimes it was impossible to calculate its concentration in these sintered steels.

Microstructure inhomogeneity of sintered steels can be confirmed by the observation that Mn concentration is different than initial 3%. Manganese concentration, e.g. at a level of 10% or 22%, shows that Mn particles are not dissolved in the microstructure (it is possible only after sintering at 1120°C). Chromium concentration in the investigated regions is somewhat higher than in the alloyed powders. Inhomogeneity of alloying elements was confirmed also by hardness measurements [37, 38, 72].

SEM investigations did not confirm any significant effect of sintering temperature and chemical composition of the sintering atmosphere on fracture of PM Mn-Cr-Mo steels. Both after low and high temperature sintering, regardless of chemical composition of the sintering atmosphere, ductile fractures were observed in the investigated steels, which is confirmed by their relatively high toughness. The fracture of low carbon steels, based both on Astaloy CrL and CrM alloyed iron powders takes place in a ductile mode. In some regions of this fracture, especially after sintering at the higher temperature, local plastic deformation can be found, which corresponds to specimen elongations above 2%. In regions in which undissolved Mn particles are present, fracture has an intergranular mode, because of oxides concentrations at grain boundaries. The role of oxide layers in the homogenisation process of chemical composition of steels has been studied in [73-74]. This phenomenon is confirmed by low toughness of the investigated steels. Mixed fracture mode - both ductile and transgranular – was found in high carbon containing steels. It is connected with the microstructure of sintered steels containing bainite and/or martensite.

The fracture investigation of PM steels show also differences in type of fracture depending on Cr and Mo concentration in the sintered steels. Low concentration of Cr and Mo in steels, irrespective of the sintering temperature and chemical composition of sintering atmosphere, result in fine grain fracture [52].

Fracture observations and their analysis depending on carbon concentration allow for conclusion that increasing the sintering temperature from 1120°C to 1250°C increases the plasticity of investigated steels. Extension the sintering time was favourable for the ductility of PM Mn-Cr-Mo steels.

The wide range of hardness of microstructural constituents can be probably connected with inhomogeneity of chemical composition of phase existed in sintered steels [31]. This phenomenon can be further investigated.

During investigations of the porosity of sintered steels it is hard to oppose the hypothesis presented in [75] which explains the mechanism of diffusion taking place between Fe and ferromanganese particles. In investigated steels micropores (original) and mesopres (which allow mass transport of Mn vapours into iron particles and are responsible for chemical composition of the microatmosphere during sintering) were observed. In original pores (micropores) water vapour and oxygen are accumulated, and, because of their small dimensions, diffusion processes play the main role in mass transport during sintering. During heating of the compact, Mn, because of its high vapour pressure, diffuses mainly because of secondary porosity existing in the steel. When the gas pressure in the pores drops below the desorption pressure at a given temperature, the desorption process of water vapour and $O_2$ from the surface of Fe particles starts. Because the concentration of $O_2$ is increasing, the content of Mn in iron solid solution decreases, but increases in the oxides.

Metallographic investigations show that average size of pores was not more than 25 μm (maximum values of pores distribution were in the range 2-4 μm). The results demonstrate the dependence of porosity of steels on the sintering temperature - the ECD distribution is more "thin" for steels sintered at 1250°C. This phenomenon can be explained in the following way – vapourising or subliming Mn vapours are trapped in the pores. In the presence of oxygen and water vapour, even in a sintering atmosphere with a low dew point, Mn vapours reacts with oxygen and Mn oxides are deposited in the pores. The secondary porosity in sintered steels begins during sublimation of the Mn particles [38, 76].

To utilise to the maximum extent the effects of sublimation, vaporization and condensation of Mn vapours, the alloy iron compacts must have mainly open pores, at least at the start of sintering, to ensure that these pores are filled by Mn vapours. The sublimation of Mn and dissolution of the ferromanganese particles at the sintering temperature takes place almost immediately. The distinction is generally between pores which contain a very low gas pressure (*voids)* and pores which contain Mn vapour at a pressure which at least balances (and may exceed) the surface tension forces (*bubbles)*. In physics of the Mn steel sintering we shall in general refer to pores, distinguishing between voids and bubbles only where necessary. However, this distinction is rarely meaningful, since it is generally very difficult to determine the gas pressure inside a cavity. The empirical dividing line between „voids" and „bubbles" is then simply that on sintering voids generally shrink while bubbles remain the same size or grow.

Dilatometric investigations determined the phase transformation temperature occurring in Mn-Cr-Mo steels during cooling from the sintering temperature [44, 76-78]. The analysis of dilatometric curves of PM Mn-Cr-Mo steels shows the influence of chemical composition of the powder mixture and processing conditions (sintering atmosphere and sintering temperature) on dimensional changes, in particular:

- the presence of manganese and carbon in base powder mixture decreases the temperature of $\alpha \rightarrow \gamma$ transformation during heating to ~ 780°C and ~ 815°C for mixtures based on pre-alloyed Astaloy CrL and Astaloy CrM iron powders, respectively;
- type of sintering atmosphere (its chemical composition) does not influence the progress of $\alpha \rightarrow \gamma$ transformation;
- the isothermal shrinkage does not depend on the chemical composition of the sintering atmosphere, but depends on the isothermal sintering temperature – the shrinkage was approx. 0.6% and 1.3% (1.4%) for compacts, sintered at 1120°C and 1250°C, respectively, based on Astaloy CrL (Astaloy CrM) powder.
- the influence of Mn and C, as elements increasing hardenability of steel, is demonstrated by dimensional changes of sintered compacts during their cooling from the sintering temperature. $\alpha \rightarrow \gamma$ transformation is visible only in compacts based on Astaloy CrL powder containing the lowest amount of carbon. After sintering at 1120°C, bainitic transformation starts at ~470 and ~460°C, for steels based on Astaloy CrL and Astaloy CrM powders, respectively. Increasing the sintering temperature increases $B_s$ temperature by about 40°C. $B_s$ temperature of steels sintered in argon, irrespective of chemical composition and isothermal sintering temperature, is about 20°C higher than $B_s$ temperature for other steels;
- steels containing the highest amount of carbon show increased hardenability such that during relatively slow cooling rate (0.3°C/s) the only effect recorded on dilatometric curves during cooling is the effect of the martensitic transformation. It is worth to emphasize that this effect is observed also in steels sintered at lower (1120°C) temperature.

The analysis of chemical composition of PM Mn-Cr-Mo steels processed in different conditions show [31, 48, 52, 70] that bigger loss of carbon and oxygen takes place after sintering at higher (1250°C) temperature; what is more, there is a correlation between carbon loss and oxygen concentration in the sintered materials. The reason for this could be a decarburization effect during sintering steels in the hydrogen atmosphere and also the reduction of oxides by carbon. Such mechanism was proposed in [24] with reference to Mn steels. The results of chemical analysis show the possibility of using $N_2$-rich atmospheres for production of PM Mn-Cr-Mo steels.

## CONCLUSIONS

On the basis of results obtained during the investigations, following conclusion can be drawn:

1. Mechanical properties of PM Mn-Cr-Mo steels depend on processing parameters, especially on chemical composition of powder mixture, sintering time and temperature, chemical composition of sintering atmosphere and heat treatment.
2. Unfavourable combination of mechanical and plastic properties can be improved by tempering at 200°C.
3. Investigated steels are characterised by a low friction coefficient and wear resistance, which can be useful during production of e.g. sintered gears in electromachines or in automotive industry (engine or gearbox parts).
4. Increasing the sintering time improves the mechanical properties of PM Fe-Mn-Cr-Mo-C steels, but, for economic reasons, the sintering time should not exceed 60 minutes.
5. Investigated steels had an inhomogeneous microstructure which depends on carbon concentration, sintering parameters and tempering conditions.

6. The ECD parameter of pores in investigated steels depends mainly on the size of ferromanganese particles; increasing the sintering temperature causes a narrowing of the distribution of ECD.
7. Dilatometric investigations determined the temperatures of phase transformations occurring in the investigated steels.
8. The connection between carbon and oxygen loss, taking place in the sintered steels, is probably connected with decarburization and oxide reduction by carbon.
9. Steels sintered in nitrogen atmosphere have satisfactory mechanical properties, which allow using this atmosphere during mass scale production of PM Fe-Mn-Cr-Mo-C steels. The prerequisite for high mechanical properties of these steels is their sintering under cover or with a getter at 1250°C.

**Acknowledgments**

The financial support of the Ministry of Science and Higher Education under AGH contract no 11.11.110.299 is acknowledged. The author would also like to thank Prof. A. S. Wronski for his content-related comments and editing this text.

**References**

[1] German, RM.: Powder metallurgy science. Princeton : MPIF, 1984
[2] EU Carcinogenic Directives 90/394/EEC and 91/322/EEC
[3] Mitchell, SC., Wronski, AS., Cias, A., Stoytchev, M. In: Proc. $PM^2TEC$ 1999. Vol. 3, 1999, p. 7
[4] Mitchell, SC., Wronski, AS., Cias, A.: Inżynieria Materiałowa, vol. 5, 2001, p. 633
[5] Wronski, AS., et al.: Tough, fatigue and wear resistance sintered gear wheels. Final Report on EU Copernicus Contract no ERB CIPA-CT94-0108, European Commission, 1998
[6] Sulowski, M., Cias, A.: Inżynieria Materiałowa, vol. 4, 1998, p. 1179
[7] Cias, A., Sulowski, M., Stoytchev, M. In: Proc. of 7th European Conf. on Advanced Materials and Processes - EUROMAT 2001, June 2001
[8] Keresti, R., Selecka, M., Šalak, A. In: Proc. Int. Conf. DFPM'99. Vol. 2, 1999, p. 108
[9] Mitchell, SC., Becker, BS., Wronski, AS. In: Proc. 2000 PM World Congress. Vol. 2, 2000, p. 923
[10] Cias, A., Stoytchev, M., Wronski, AS. In: Proc. 2001 Int. Conf. on Powder Metallurgy and Particulate Materials. Vol. 10, 2001, p. 131
[11] Šalak, A.: Powder Metallurgy International, vol.16, 1984, p. 6
[12] Šalak, A., Leitner G., Hermel, W.: Powder Metallurgy International, vol. 13, 1981, p. 1
[13] James, J., Lindsley, B., Rutz, B., Narasimhan, KS. In: Proc. Euro PM2009. Vol. 1, 2009, p. 23
[14] Lindsley, B., James, J. In: Proc. 2010 PM World Congress&Exhibition. Vol. 3. Sintered steels, 2010, p. 151
[15] Bergman, O., Bengtsson, S. In: Euro PM2009, Sintered Steels II – Sinterhardening
[16] Dudrova, E., Kabatova, M., Bidulsky, R., Wronski, AS.: Powder Metall., vol. 47, 2004, no. 2, p. 181
[17] Bidulský, R., Grande, M-A. In: Proc. PM2010 World Congress. Vol. 3. Sintered Steels: Mechanical Properties, 2010, p. 95
[18] Hryha, E., Nyborg, L., Dudrova, E., Bengtsson, S. In: Proc. Euro PM2009. Sintered Steels 1 – Composition
[19] Hryha, E. In: Proc. Euro PM2013. Vol. 2. Sintering – Atmospheres and Atmosphere Control, p. 333

[20] Hryha, E. In: Euro PM2013. Vol. 2. Sintering – Fundamentals and Modelling, p. 303
[21] Gierl-Mayer, C. In: Proc. Euro PM2013. Vol. 3. Sintered Steels – Fatigue and Durability, p. 397
[22] Ciaś, A.: Science of Sintering, vol. 47, 2015, no. 1, p. 61
[23] Metalog guide, Struers A/S, 1992
[24] Ciaś, A., Mitchell, SC., Pilch, K., Ciaś, H., Sułowski, M., Wronski, AS.: Powder Metall., vol. 46, 2003, no. 2, p. 165
[25] Ciaś, A., Mitchell, SC., Wronski, AS. In: Proc. Euro PM2004. Vol. 2. Sintering - Secondary and finishing operations, p. 5
[26] Ciaś, A., Mitchell, SC., Watts, A., Wronski, AS.: Powder Metallurgy, vol. 42, 1999, no. 3 p. 227
[27] Mitchell, SC., Wronski, AS., Ciaś, A., Stoytchev, M. In: Proc. DF PM'99 - Deformation and Fracture in structural PM materials. Vol. 1, 1999, p. 1
[28] Ciaś, A., Mitchell, SC.: Powder Metallurgy Progress, vol. 5, 2005, no. 2, p. 82
[29] Hryha, E., Nyborg, L.: Powder Metall., vol. 57, 2014, no. 4, p. 245
[30] Sułowski, M., Ciaś, A.: Arch. Metall. Mater., vol. 49, 2004, no. 1, p. 55
[31] Sułowski, M.: Arch. Metall. Mater., vol. 49, 2004, no. 3, p. 641
[32] Sułowski, M.: Arch. Metall. Mater., vol. 50, 2005, no. 4, p. 827
[33] Ducket, R., Robin, DA.: The International Journal of Metals and Materials, vol. 74, 1966, no. 444, p. 163
[34] Esper, FJ., Friese, K-H., Zeller, R.: International Journal of Powder Metallurgy, vol. 5,1969, no. 3, p. 19
[35] Chatterjee, SK., Castell-Evans, JV., Ainsworth, PA.: Powder Metallurgy, vol. 15, 1972, no. 30, p. 153
[36] Chatterjee, SK., Mackay, CA.: Powder Metall., vol. 23, 1980, no. 4, p. 183
[37] Sułowski, M.: Arch. Metall. Mater., vol. 2, 2006, no. 51, p. 227
[38] Sułowski, M., Dudek, P.: Arch. Metall. Mater., vol. 53, 2008, no. 3, p. 827
[39] SigmaScan Pro - http://www.sigmaplot.com/products/sigmascan/sigmascan.php, 18.09.2015
[40] Goetzl, GC.: Treatise on powder metallurgy. New York-London : Intersci. Publ., 1950
[41] Kovachev, B., Mihovski, M., Stoytchev, M., Sulowski, M.: Arch. Metall. Mater., vol. 1, 2007, no, 52, p. 97
[42] Sulowski, M.: Arch. Metall. Mater., vol. 52, 2007, no. 4, p. 617
[43] Sułowski, M., Faryj, K.: Arch. Metall. Mater., vol. 54, 2009, no. 1, p. 121
[44] Ciaś, A., Sułowski, M.: Arch. Metall. Mater., vol. 54, 2009, no. 4, p. 1093
[45] Ciaś, A.: Development and Properties of Fe-Mn-(Mo)-(Cr)-C Sintered Structural Steels. Krakow : AGH – Uczelniane Wydawnictwa Naukowo-Dydaktyczne, 2004
[46] Sułowski, M., Ciaś, A.: Arch. Metall. Mater., vol. 56, 2011, no. 2, p. 293
[47] Sułowski, M.: Powder Metall., vol. 53, 2010, no. 2, p. 125
[48] Pieczonka, T., Sułowski, M., Cias, A.: Arch. Metall. Mater., vol. 57, 2012, no. 4, p. 1001
[49] Sułowski, M., Ciaś A., Pieczonka, T.: Arch. Metall. Mater., vol. 59, 2014, no. 2, p. 575
[50] Sulowski, M.: Arch. Metall. Mater., vol. 59, 2014, no. 4, p. 1499
[51] Sulowski, M., Kulecki, P., Radziszewska, A.: Arch. Metall. Mater., vol. 59, 2014, no. 4, p. 1506
[52] Sulowski, M., Kabatova, M., Dudrova, E.: Powder Metallurgy Progress, vol. 12, 2012, no. 2, p. 71
[53] Mitchell, SC., Cias, A.: Powder Metallurgy Progress, vol. 4, 2004, no. 3, p. 132
[54] Šalak, A., Selecká, M., Bureš, P.: Powder Metallurgy Progress, vol. 1, 2001, no. 1, p.41

[55] Sulowski, M., Cias, A., Pieczonka, T. In: Proc. 6th International Powder Metallurgy Conference and Exhibition. Ankara, Turkey, 2011, p. 177
[56] Sulowski, M., Cias, A. In: Proc. 2010 PM World Congress. Vol. 3. Sintered steels, 2010, p. 103
[57] Cias, A., Mitchell, SC., Wronski, AS. In: Proc. PM 2004 World Congress & Exhibition. Vol. 2, 2004, p. 1
[58] Pieczonka, T., Georgiev, J., Stoytchev, M., Mitchell, SC., Teodosiev, D., Gyurov, S.: Powder Metallurgy Progress, vol. 4, 2004, no. 4, p. 211
[59] Wronski, AS., Cias, A.: Powder Metallurgy Progress, vol. 3, 2003, no. 3, p. 119
[60] Ciaś, A.: Powder Metallurgy, vol. 56, 2013, no. 3, p. 231
[61] Ciaś, A.: International Journal of Materials Research, vol. 106, 2015, no. 5, p. 494
[62] Salak, A.: Powder Metallurgy International, vol. 18, 1986, no. 4, p. 266
[63] Hoganas Handbook for Sintered Components. Part 2: Production of sintered components. Hoganas AB 1997, p. 6
[64] Schatt, W., Wieters, K-P.: Powder Metallurgy – Processing and Materials, EPMA, 1997, p. 165
[65] Sulowski, M., Cias, A., Frydrych, H., Frydrych, J., Olszewska, I., Golen, R., Sowa, M.: Materials Science Forum, vol. 534-536, 2007, no. 1, p. 757
[66] Sułowski, M.: Ores and Non-Ferrous Metals , vol. 53, 2008, no. 2, p. 103
[67] Technical report from grant: „Struktura i własności mechaniczne spiekanych stali konstrukcyjnych z dodatkiem manganu, chromu i molibdenu, wytwarzanych w atmosferze azotu", Krakow, December 2007
[68] Sułowski, M., Matusiewicz, P.: Inżynieria Materiałowa, 2008, no 4, p. 258
[69] Sulowski, M., Matusiewicz, P.: Stereology and Image Analysis in Material Science, Solid State Phenomena, vol. 197, 2013, p. 33
[70] Sulowski, M., Kabatova, M., Dudrova, E.: Powder Metallurgy Progress, vol. 11, 2011, no. 1-2, p. 132
[71] Fiał, C., Dudrova, E., Kabatova, M., Kupková, M., Selecka, M., Sulowski, M., Cias, A.: Powder Metallurgy Progress, vol. 14, 2014, no. 3, p. 137
[72] Sulowski M.: Powder Metallurgy Progress, vol. 7, 2007, no. 2, p. 80
[73] Hryha E., Dudrova E. In: Application of Thermodynamics to Biological and Materials Science, www.intechopen.com/articles/show/title/the-sintering-2011, p. 573
[74] Hryha E. Dudrova, E.: Materials Science Forum, vol. 534-536, 2007, p. 761
[75] Hrubovcakova, M., Dudrova, E., Hryha, E., Kabatova, M. and Harvanova, J.: Advances in Materials Science and Engineering, vol. 2013, 2013, Article ID 789373
[76] Ciaś, A., Sułowski, M., Frydrych, H., Frydrych, J. In: Proc. PM2TEC Montreal. Part 7 – Materials, 2005, p. 31
[77] Sulowski, M., Cias, A., Frydrych, H., Frydrych, J., Olszewska, I., Golen, R., Sowa, M. In: Proc. PowderMet2006 International Conference. 2006, p. 10-114
[78] Sulowski, M. In: Proc. DFPM 2005. 2005, p. 308